ACS APPLIED MATERIALS & INTERFACES

Research Article

www.acsami.org

Binding Energy and Work Function of Organic Electrode Materials Phenanthraquinone, Pyromellitic Dianhydride and Their Derivatives Adsorbed on Graphene

Yang-Xin Yu*

Laboratory of Chemical Engineering Thermodynamics, Department of Chemical Engineering, Tsinghua University, Beijing 100084, People's Republic of China

State Key Laboratory of Chemical Engineering, Tsinghua University, Beijing 100084, People's Republic of China

Supporting Information

ABSTRACT: Electroactive organic compounds are a novel group of green cathode materials for rechargeable metal-ion batteries. However, the organic battery life is short because the organic compounds can be dissolved by nonaqueous electrolytes. Here a comparative investigation of phenanthraquinone (PQ), pyromellitic dianhydride (PMDA) and their derivatives, i.e., benzo[1,2-b:4,3-b′]difuran-4,5-dione (BDFD), benzo[1,2-b:4,3-b′]dithiophene-4,5-quinone (BDTQ), 3,8-phenanthroline-5,6-dione (PAD), pyromellitic dithioanhydride (PMDT), pyromellitic diimide (PMDI) and 1,4,5,8-anthracenetetrone (ATO), adsorbed on graphene is performed using a density functional theory (DFT) with a van der Waals (vdW) dispersion-correction. The computed results show a strong physisorption with the binding energies between 1.10 and 1.56 eV. A sequence of the calculated binding energies from weak to strong is found to be BDFD < BDTQ < PMDA ≤ PMDI < PMDT < PQ < PAD < ATO. The formation of stable organic molecule−graphene nanocomposites can prevent the dissolution of the eight organic compounds in nonaqueous electrolyte and hence improve cycling performance of batteries. In addition, the work functions for the nanocomposites are found to be strongly affected by the work function of each organic compound. To understand the DFT results, a novel simple expression is proposed to predict the work function of the nanocomposites from the interfacial dipole and the work functions of the isolated graphene nanosheet and organic molecules. The predicted work functions for the nanocomposites from the new equation agree quite well with the values calculated from the vdW dispersion-corrected DFT.

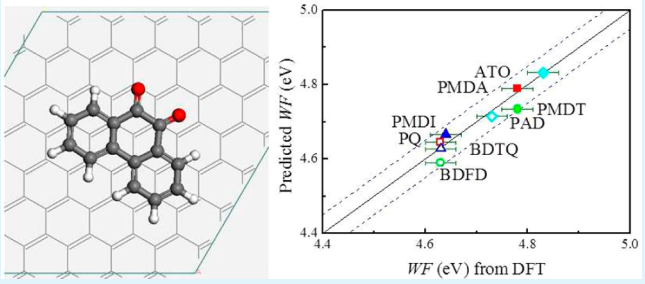

KEYWORDS: *graphene, electroactive organic compound, first-principles, adsorption, work function*

INTRODUCTION

In the past decade, much attention has been focused on rechargeable lithium-ion batteries because they have gained widespread adoption as energy storage devices.[1,2] A lithium-ion battery is typically made up of a cathode, an anode and an electrolyte made of a lithium salt and an organic solvent. Electrodes are the key part of the batteries and thus the electrode materials are one of the most important elements influencing the electrochemical performance of these batteries. In traditional lithium-ion batteries, lithium transition-metal oxides, which can reversibly store lithium ions, are selected as cathode materials, and pristine or N-doped graphene materials are used as the anode.[3] However, transition metals are regarded as important toxic pollutants and many researchers have investigated their accumulation in eco-systems.[4−6] More seriously, extensive use of transition-metals such as copper, nickel, manganese, cobalt, etc. in batteries will result in not only the environmental pollution but also rapid depletion of primary resources.[7] "Green electrodes" are expected to be explored to solve these problems. Organic batteries have promise to surpass present lithium-ion batteries in terms of safety, environmental protection and resource price.[7,8]

Organic electrode materials contain a functional group of quinone, anhydride, or nitroxide radical. Most of them perform very well at the first cycle, but only a very limited battery cycle life can be obtained due to their significant solubility in the electrolyte. Several approaches have been attempted to solve the dissolution problem. A reasonable way seems to be the construction of polymer electrode materials. However, only a marginal improvement can be achieved in this way because the polymeric electrode material has almost the same solubility in nonaqueous electrolyte as its monomer. This is because the solubility parameters of the polymer and its monomer are very near in terms of group contribution methods, considering the volume change is not too large during the polymerization. This conclusion does not violate the famous Flory−Higgins theory

Received: July 9, 2014
Accepted: September 4, 2014
Published: September 12, 2014

because the Flory–Higgins parameters are usually evaluated from the solubility parameters. For example, a polymeric quinone from electrochemically synthesized poly(1,4-dimethoxybenzene) exhibits a really disappointing cycling performance.[9] A stable and inactive skeleton therefore has to be introduced to the polymer chain. Nonetheless the theoretical specific capacity will be reduced and the ion/electron transfer rate in the electrode will be slowed down. Besides the usage of an alternative electrolyte, incorporating mesoporous carbon as well as a functionalized graphene nanocomposite can strengthen the immobilization and improve the cycling performance by preventing the unexpected dissolution of the organic active material.[10] Specially, the organic nanocomposite with highly dispersed graphene can also improve the charge/discharge rate capability of organic cathode materials.

It is known from the thermodynamic principle that the extent of the reduction of solubility of organic electrode material in the nanocomposite depends strongly on the interaction between the organic compound and graphene. On the other hand, the strong interaction between the organic compound and graphene lowers the dissolution rate of organic molecules because an additional energy barrier of desorption from graphene is required in the dissolution process. In a previous investigation,[11] the stability of nanocomposites composed of four organic compounds and graphene or h-BN was evaluated using a density functional theory with a van der Waals (vdW) dispersion correction (vdW-DFT), and the strong physical interaction between the organic molecules and graphene or h-BN results in a reduction of solubility of the four organic compounds in electrolytes. This conclusion was directly validated by experimental results of Liang et al.[12] and indirectly verified by Song et al.[10] The success of the vdW-DFT inspires us to continue the investigation on the interactions between some more organic battery active materials and graphene.

A strong adsorption of an organic molecule on graphene can induce work function shift compared with pristine graphene. The work function shift plays an important role in electrochemistry[13] and can be used as a means to improve the performance of fluorescent lamp cathode surfaces.[14] More theoretical studies on work function of nanocomposites are needed to establish a quantitative understanding on the work function change induced by adsorption of organic molecules on graphene.

As having been validated in previous investigations, ab initio DFT is a very powerful tool for predicting thermodynamic and electrochemical properties of battery active materials.[15] For organic molecules on graphene, nonlocal dispersion correlations are important and a vdW dispersion-corrected DFT proposed by Grimme[16] (DFT-D) has proven to be accurate for the prediction of the inter- and intramolecular noncovalent interactions. In this work, the DFT-D was selected to investigate the adsorption of phenanthraquinone (PQ), pyromellitic dianhydride (PMDA) and their derivatives, i.e., benzo[1,2-b:4,3-b′]difuran-4,5-dione (BDFD), benzo[1,2-b:4,3-b′]dithiophene-4,5-quinone (BDTQ), 3,8-phenanthroline-5,6-dione (PAD), pyromellitic dithioanhydride (PMDT), pyromellitic diimide (PMDI) and 1,4,5,8-anthracenetetrone (ATO), on monolayer graphene. These molecules are environmentally friendly materials due to that they could be produced and recycled both easily and cheaply, only exerting a minimal burden on the environment. They perform very well as a cathode because the organic redox mechanisms have very fast reaction kinetics. In the meantime, they all suffer the problem of dissolution in the electrolyte, which significantly affects their cycling stabilities. Therefore, they were selected for study to reduce their solubility in electrolytes. The binding energies and work functions of these compounds were computed and analyzed in detail. The DFT-D calculation method used in this work is similar to the previous work.[11] Different from the previous work,[11] the thermodynamic properties of eight new organic compounds with anhydride or nonrational-symmetric quinone groups were theoretically investigated by introducing monolayer graphene and a novel simple equation for work function of the organic compound–graphene nanocomposites was proposed based on the work function of the organic molecules and the interfacial dipole density. The proposed equation well reproduces the work function data obtained from ab initio DFT.

COMPUTATIONAL DETAILS

Spin-polarized ab initio DFT calculations were carried out using the DMol^3 package,[17,18] similar to the previous work.[11] The generalized gradient approximation (GGA) with the PBE functional[19] and the hybrid GGA with the B3LYP functional[20] were used to obtain the electronic structures and energies of the systems studied. Two cases were considered in the calculations in order to emphasis the importance of dispersive interactions between atoms. One case is using the PBE functional only and another case is using the DFT with a vdW dispersion-correction. In the geometry optimization process, a vdW-DFT with the parameters determined by Grimme[16] was used in the case that the vdW-dispersion interaction needs to be included. A careful explanation how dispersion correction was implemented in the Dmol^3 DFT package can be found in the previous work.[11] It is sufficiently reliable for the purpose of this work. Periodical boundary condition was applied to *x*-, *y*- and *z*-directions in the geometric structure optimization calculations.

The ground state energies for the neutral, cationic and anionic forms of each organic compound were computed for one molecule using the PBE and B3LYP functional with the dispersion correction (i.e., PBE-D and B3LYP-D).[16] Here nonperiodic boundary condition was applied. The ionization energy (IE) and electron affinity (EA) can be evaluated from the energies of different forms of each organic compound

$$\mathrm{IE} = E_{M+} - E_{M} \quad (1)$$

$$\mathrm{EA} = E_{M} - E_{M-} \quad (2)$$

where E_M, E_{M+} and E_{M-} represent the energies of the neutral, cationic and anionic forms of each organic molecule studied, respectively.[21]

The binding energy (E_b) and work function (WF) can be estimated in the same way as in the previous work.[11,22] Because the ionization energy and electron affinity are dominated by band structure terms, they can be alternatively defined as energy differences IE = $E_{vac} - E_{HOMO}$ and EA = $E_{vac} - E_{LUMO}$, where E_{vac}, E_{HOMO} and E_{LUMO} are the energies of a vacuum level, HOMO and LUMO states, respectively. Assuming that a Fermi level is located in the midplane of the HOMO and LUMO levels, the work function can be simply written as the form of WF = (IE + EA)/2.

RESULTS AND DISCUSSION

Ionization Energy and Electron Affinity. The molecular structures of the eight organic electrode materials are displayed in Figure 1. Each organic compound shown in Figure 1 contains an electrochemical functional group of quinone or anhydride. Although the PBE functional appears to outperform over the B3LYP functional based on the HOMO–LUMO gap data of ten molecules with the sizes ranging from diatomic molecules to those consisting of up to three benzene rings,[23] their performance has not been validated for the molecules

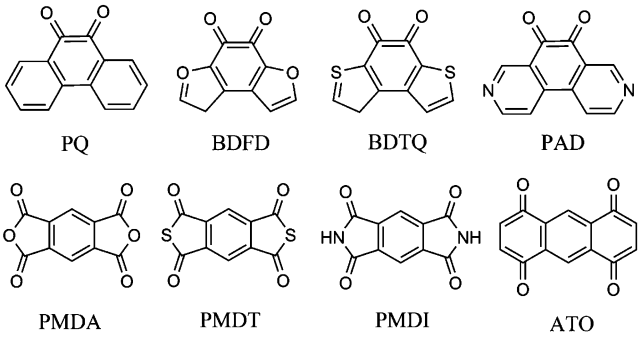

Figure 1. Molecular structures of the eight organic molecules studied in this work.

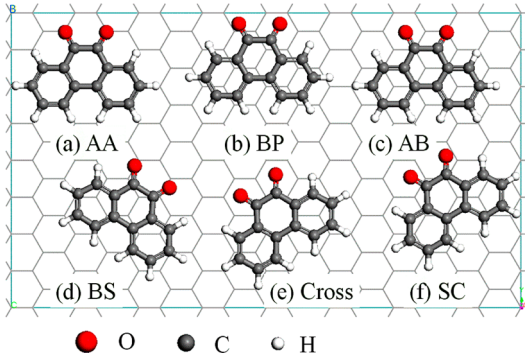

Figure 2. Studied adsorption configurations of a PQ molecule on a graphene nanosheet.

containing either quinone or anhydride groups. It is necessary to compare the reliability of the PBE and B3LYP results for the PQ, PMDA and their derivatives studied in this work. The IE and EA for the eight organic compounds have been calculated and are listed in Table 1. To validate the calculated results and show the phase state of the organic materials, available experimental data[24−28] of IE, EA and melting points are also included in Table 1. We can find in Table 1 that the B3LYP-D scheme predicts very accurate IE whereas it substantially underestimates the EA. The PBE-D scheme underestimates the IE and slightly overestimates the EA. Because the work function is approximately the average value of the IE and EA, the PBE-D scheme is expected to predict a reasonable work function. This has been validated for graphene in the previous work.[11] The WF for each organic compound listed in Table 1 was calculated in a same way as in the previous work.[11] As can be found in Table 1, the values of the WF are slightly different from those of (IE + EA)/2. This is because different conditions are used in the calculations of WF and of IE and EA. The calculated work functions for the eight organic electrode materials are in the following order: PQ < BDTQ < BDFD < PAD < PMDI < ATO < PMDT < PMDA. They are in the range of 4.93−6.21 eV, and all of them are larger than the work function of the pristine graphene (4.49 eV).

Binding Energy. The results from the PBE scheme were compared with those from the PBE-D scheme in order to emphasize the importance of the vdW dispersion. All possible adsorption configurations for eight organic molecules on graphene were systematically investigated in this work and the six representative adsorption configurations are shown in Figure 2. The six kinds of adsorption sites in Figure 2 are labeled as AA-stacking (AA), bridge-parallel (BP), AB-stacking (AB), bridge-slant (BS), Cross and shifted Cross (SC) configurations, respectively. The definition of each configuration has been described in detail in the previous work.[11] It should be pointed out that there are two adsorption configurations on both the BS and SC sites due to the distinguishable carbon atoms in the middle benzene ring. In these cases, only the adsorption configurations with the lower energy as displayed in Figure 2d,f were recorded for the estimation of the geometric parameters, binding energies and work functions.

The calculated binding energies (E_b) for the PQ, BDTQ, BDFD, PAD, PMDA, PMDT, PMDI and ATO molecules on graphene are listed in Table 2. It is interesting to find that the binding energy of the BDFD molecule on the AB site is the same as that on the BP site when the vdW dispersion was included in the calculation. In other words, adsorption configurations of the BDFD molecule on both the AB and BP sites are stable, suggesting the coexistence of the AB and BP configurations on a graphene nanosheet. The PQ and PAD molecules prefer to be adsorbed on the AB site of graphene and the BDTQ, PMDA, PMDT, PMDI and ATO molecules favor the BP site. The binding energy of the PQ BDFD, BDTQ and PAD molecules on the AA site is the smallest one. In contrast, the binding on the Cross adsorption site may be the weakest for the PMDA, PMDT, PMDI and ATO molecules on a graphene nanosheet. The most stable adsorption configurations for the PQ, BDFD, BDTQ and PAD molecules are illustrated in Figure 3. Figure 4 depicts the most stable adsorption geometries for the PMDA, PMDT, PMDI and ATO molecules on graphene.

Table 1. Melting Point, Ionization Energy and Electron Affinity for the Organic Compounds Studied

		IE (eV)[a]		EA (eV)[a]		
compound	melting point (K)	PBE-D	B3LYP-D	PBE-D	B3LYP-D	WF (eV)[b]
PQ	481.15 ± 4[c]	8.10	8.64	1.98	1.51	4.93
			8.64 ± 0.03[d]		1.83[d]	
BDFD		8.32	8.80	1.92	1.53	5.03
BDTQ		8.14	8.55	2.06	1.68	5.02
PAD	>583.15[e]	8.05	8.98	2.64	2.04	5.31
PMDA	560.15[f]	9.93	10.94	2.90	2.49	6.21
PMDT		9.19	10.03	2.93	2.49	5.91
PMDI	723−727[g]	9.06	10.06	2.34	1.94	5.55
ATO		8.61	9.79	3.00	2.34	5.71

[a]Uncertainty from DFT is ±0.005 eV. [b]Uncertainty from DFT is ±0.03 eV. [c]Experimental data from Pitt and Smyth.[24] [d]Experimental data from Potapov and Sorokin.[25] [e]Experimental data from Botana et al.[26] [f]Experimental data from Sakai.[27] [g]Experimental data from Lawton and McRitche.[28]

Table 2. Calculated Binding Energy (in eV) for the PQ, BDFD, BDTQ, PAD, PMDA, PMDT, PMDI and ATO Molecules on a Graphene Nanosheet[a]

adsorbate	DFT	AA	BP	AB	BS	Cross	SC
PQ	PBE	0.273	0.279	0.279	0.259	0.268	0.279
	PBE-D	1.174	1.304	1.308	1.272	1.286	1.304
BDFD	PBE	0.242	0.254	0.256	0.255	0.252	0.253
	PBE-D	0.994	1.095	1.095	1.085	1.086	1.083
BDTQ	PBE	0.247	0.254	0.257	0.255	0.256	0.257
	PBE-D	1.030	1.148	1.139	1.140	1.131	1.136
PAD	PBE	0.285	0.293	0.293	0.284	0.294	0.297
	PBE-D	1.166	1.314	1.318	1.292	1.309	1.289
PMDA	PBE	0.267	0.280	0.276	0.272	0.254	0.264
	PBE-D	1.086	1.201	1.155	1.167	1.067	1.128
PMDT	PBE	0.266	0.278	0.275	0.269	0.255	0.263
	PBE-D	1.125	1.279	1.209	1.217	1.131	1.168
PMDI	PBE	0.219	0.238	0.231	0.233	0.220	0.223
	PBE-D	1.088	1.206	1.148	1.173	1.076	1.130
ATO	PBE	0.325	0.345	0.338	0.332	0.323	0.327
	PBE-D	1.327	1.564	1.434	1.468	1.354	1.393

[a]Uncertainty is ±0.001 eV.

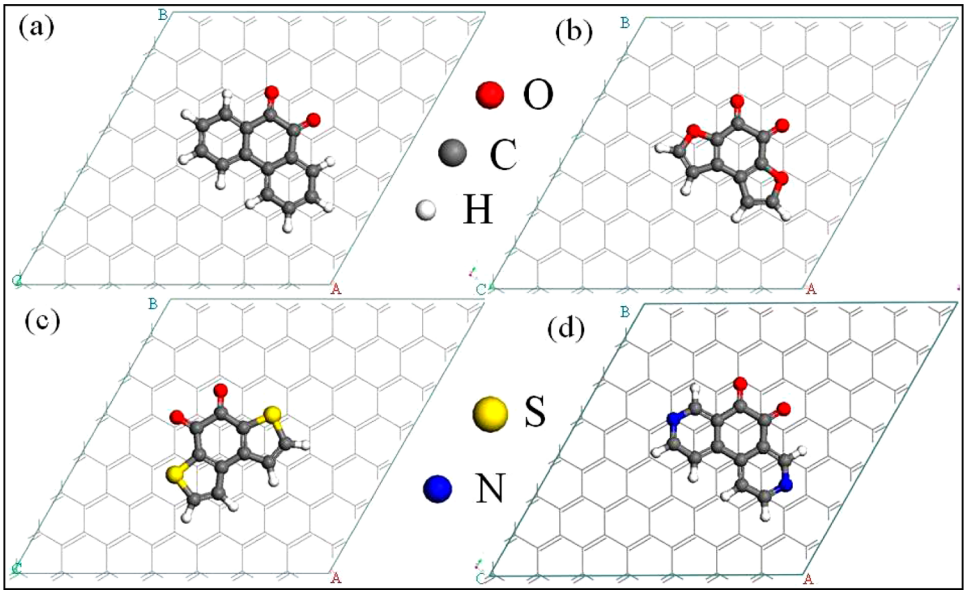

Figure 3. Equilibrium adsorption geometries of (a) PQ, (b) BDFD, (c) BDTQ and (d) PAD molecules on monolayer graphene.

The optimized geometric structures of the eight molecules on the AA, AB, BP, BS, Cross and SC adsorption sites are illustrated in Figures S1−S8 (Supporting Information). It is worth noting that all the geometric structures shown in Figures 3, 4 and S1−S8 (Supporting Information) were obtained using the PBE-D scheme. A sequence of binding energies for the eight organic compounds on a graphene nanosheet is found to be PMDI < BDFD ≤ BDTQ < PMDT ≤ PQ ≤ PMDA < PAD < ATO using the PBE scheme and BDFD < BDTQ < PMDA ≤ PMDI < PMDT < PQ < PAD < ATO using the PBE-D scheme. It is found that the positions of the molecules with a functional group of anhydride (PMDA, PMDT and PMDI) in the sequence are changed when the vdW dispersion is considered in the calculation. Because there is no other interaction involved in the two schemes, the vdW dispersion is the only interaction responsible for the difference in the binding energy sequence from the two schemes.

The most stable adsorption configurations for the BDTQ and PAD molecules are on the SC site of graphene when the vdW-dispersion is not corrected. It is the vdW dispersion that makes the BDTQ and PAD molecules adsorbed most stable on the BP and AB sites, respectively. However, the vdW dispersion is not the cause of the stable BP and AB configurations for the other six organic molecules because the same most stable configuration on a graphene nanosheet is obtained from the two schemes. Perhaps it is due to the symmetry of the polarized bonds (C═O) and the higher terms of electrostatic interactions. It seems to be true that quinone molecules with rotational symmetry, such as PMDA, PMDT, PMDI, ATO and the four quinones studied in the previous work,[11] favor the BP site of a graphene nanosheet.

The adsorption height (d_z) for the eight organic compounds are listed in Table 3. Here the adsorption height is actually a vertical distance which is an average value of the distances between each atom of the molecule and the graphene planar

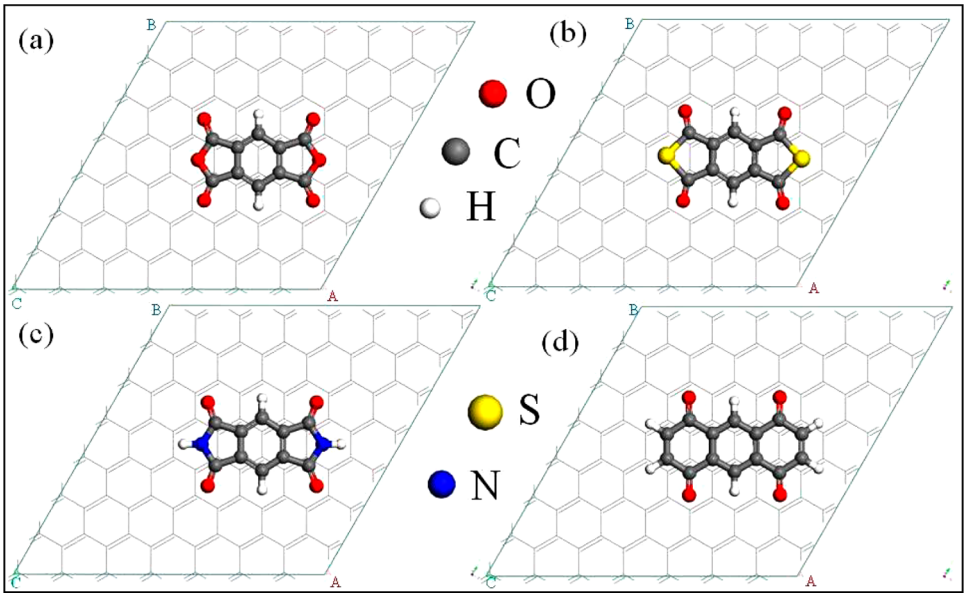

Figure 4. Equilibrium adsorption geometries of (a) PMDA, (b) PMDT, (c) PMDI and (d) ATO molecules on monolayer graphene.

Table 3. Work Function, Vertical Distance and Interfacial Dipole Moment for the Preferred Adsorption Configuration

		WF (eV)[a]		d_z (Å)[b]		$-p_z$ (D)[c]	
adsorbate	adsorption site	PBE	PBE-D	PBE	PBE-D	PBE	PBE-D
PQ	AB	4.58	4.63	3.88	3.14	0.54	0.69
BDFD	AB	4.58	4.63	3.76	3.12	0.41	0.24
BDTQ	BP	4.57	4.63	3.98	3.20	0.13	0.45
PAD	AB	4.70	4.73	3.79	3.11	0.85	0.82
PMDA	BP	4.80	4.78	3.67	3.08	0.74	0.57
PMDT	BP	4.80	4.78	3.75	3.13	0.21	0.19
PMDI	BP	4.65	4.64	3.70	3.08	0.33	0.26
ATO	BP	4.82	4.83	3.64	3.04	1.16	1.20

[a]Uncertainty is ±0.03 eV. [b]Uncertainty is ±0.005 Å. [c]Uncertainty is ±0.025 D.

layer. The obtained values of the adsorption heights are ranging from 3.64 to 3.98 Å with the PBE scheme and from 3.04 to 3.20 Å with a vdW-correction. Table 3 shows that the adsorption heights are very near for different adsorption configurations of each organic molecule using the same scheme though the binding energies are apparently different. The vdW interaction shortens the equilibrium vertical distance by 0.59−0.78 Å and enhances the attraction between the organic substances and the monolayer graphene. The lower binding energies and relatively larger vertical distances calculated using the PBE scheme indicates that the $\pi-\pi$ stacking interactions in the organic compound-graphene composites are substantially underestimated by it.

To demonstrate the important role of the vdW dispersion, the binding energy resulted from the vdW dispersion ($E_{b,vdW}$) was obtained by subtracting the PBE part ($E_{b,PBE}$) from the total binding energy ($E_{b,PBE-D}$). The obtained values of $E_{b,vdW}$ for the six adsorption sites of the eight organic electrode materials are displayed in Figure 5. It can be seen from Figure 5 that the most stable configuration for each molecule on monolayer graphene corresponds to the maximum $E_{b,vdW}$. Figure 5 shows that the vdW dispersion contributes the smallest value to the binding energy for the AA configuration of all the organic compounds studied. The above conclusion is in good agreement with that drawn from the AQ and derivatives adsorbed on monolayer graphene.[11] The contribution of the

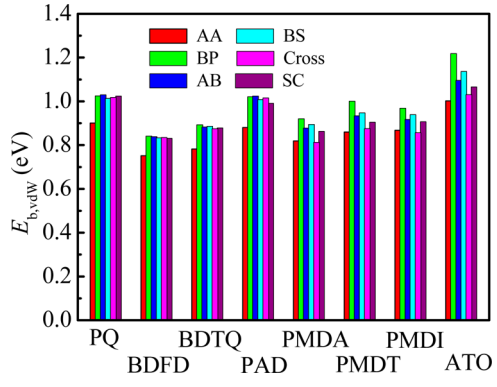

Figure 5. Calculated vdW dispersion contribution to the binding energy.

vdW dispersion is in the range of 0.84−1.20 eV, showing a strong physisorption. The magnitude of the vdW dispersion energy is the same as that in a semiempirical force field. For instance, the vdW dispersion contribution to the E_b from the DFT-D scheme is 1.029 eV for the PQ−graphene system and that from the pcff force field is 1.095 eV. The vdW dispersion contribution to the binding energy for the most stable adsorption configuration is in the following order: BDFD < BDTQ < PMDA < PMDI < PMDT < PQ ≈ PAD < ATO,

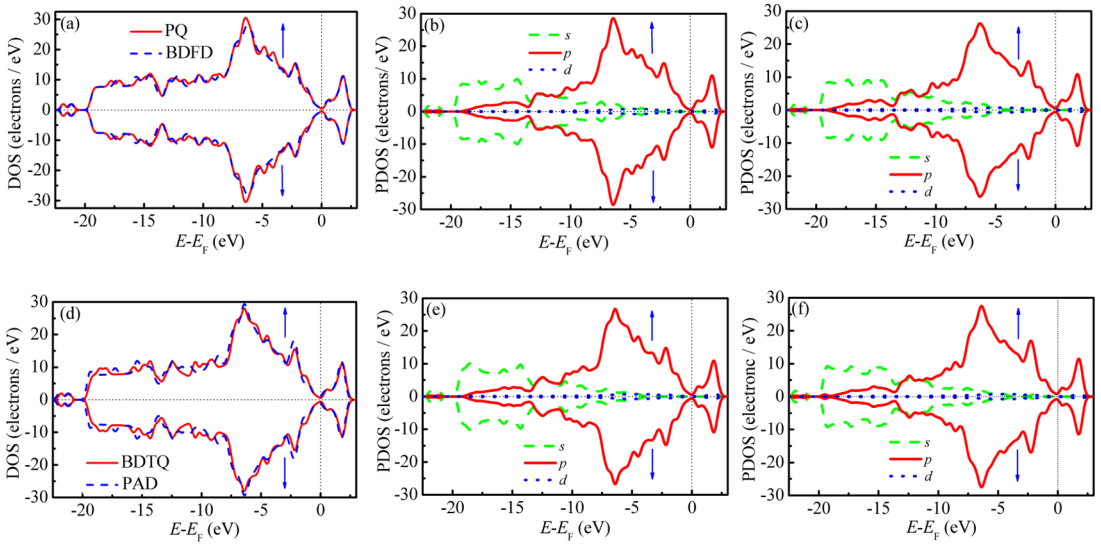

Figure 6. DOS and projected DOS (PDOS) for the preferred adsorption sites: (a) PQ and BDFD, (b) PQ, (c) BDFD, (d) BDTQ and PAD, (e) BDTQ and (f) PAD. The up and down arrows in the figure represent spin states.

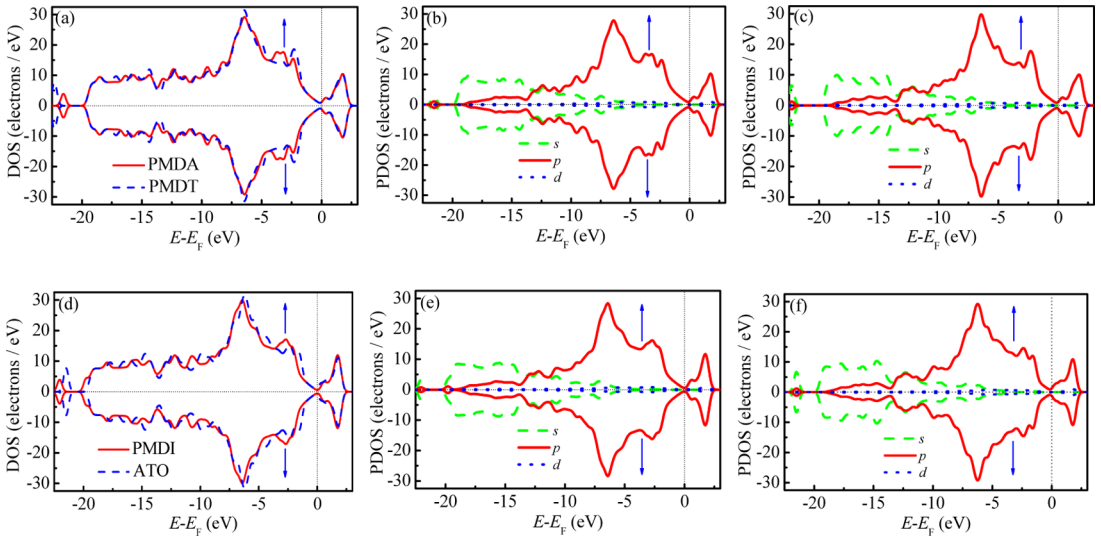

Figure 7. DOS and projected DOS (PDOS) for the preferred adsorption sites: (a) PMDA and PMDT, (b) PMDA, (c) PMDT, (d) PMDI and ATO, (e) PMDI and (f) ATO. The up and down arrows have the same meaning as in Figure 6.

which is almost the same as that for the binding energy calculated with the vdW dispersion correction. The adsorption of the ATO molecule on graphene is the strongest among the eight organic molecules studied in this work, showing that the polarized quinone group (C═O) contributes much more to the binding energy than the anhydride group. The vdW dispersion contributes to 76.6−80.3% of the total attractive interaction for the eight organic molecule−graphene nanocomposites considered. The other contributions to the binding energy may come from the differences of the kinetic, electrostatic, exchange-correlation and spin polarization energies of the corresponding systems.

The electronic DOS for the PQ, BDFD, BDTQ and PAD molecules and for the PMDA, PMDT, PMDI and ATO molecules adsorbed on the graphene nanosheet are demonstrated in Figures 6 and 7, respectively. From the observation of the DOS for the eight organic compound−graphene nanocomposites studied in this work and those investigated in the previous work,[11] it can be concluded that the higher DOS, the stronger attractive force between the organic molecule and the monolayer. For example, from Figure 6, one can find that the densities of state for the PQ and PAD molecules on graphene are higher than those for the BDFD and BDTQ molecules, respectively. And correspondingly, the binding energies of the PQ and PAD molecules on graphene listed in Table 2 are larger than those of the BDFD and BDTQ molecules, respectively.

From the viewpoint of surface-solution equilibrium, the organic substance in its pure state, μ_i^s(pure), and the saturated solutions, μ_i^L(solution), should have a same chemical potential, i.e., μ_i^s(pure) = μ_i^L(solution). The strong physisorption of the eight organic electrode materials on graphene can substantially lower the chemical potential of the materials. When graphene is introduced to the organic substance, the chemical potential of the organic substance will reduce to μ_i^s(nanocomposite), i.e., $\Delta\mu_i^s = \mu_i^s(\text{nanocomposite}) - \mu_i^s(\text{pure}) < 0$. The stronger binding energy is, the lower the $\Delta\mu_i^s$. The solubility reduction can be expressed as $\Delta \ln S = \ln(S^{\text{nanocomposite}}/S^{\text{pure}}) \propto \Delta\mu_i^s \propto -E_b$, where $S^{\text{nanocomposite}}$ and S^{pure} are the solubility of the

dx.doi.org/10.1021/am504452a | ACS Appl. Mater. Interfaces 2014, 6, 16267−16275

organic−graphene nanocomposite and pure organic compound, respectively. Thus, binding energy is directly related to the reduction of the solubility for each organic compound. Therefore, the introduction of graphene to the eight organic electrode materials to form organic molecule−graphene nanocomposites can reduce their solubility in nonaqueous electrolyte and achieve an improved cycling stability when they are used as a cathode material. Furthermore, the introduction of graphene to the organic compounds enhances the electronic conductivity, and thus makes charging and discharging ultrafast. There are evidence available that shows these electrode material can still have reasonably high capacity in comparison to transition-metal materials. For instance, the benzofuro[5,6-b]furan-4,8-dione (BFFD)−graphene nanocomposite electrode possesses an experimental energy density of approximately 560 W h kg^{-1} after 100 cycles.[12] This is higher than that of typical transition-metal materials such as commercial cobalt acid lithium (~550 W h kg^{-1}). This method is efficient as has been validated in the two recent experiments.[10,12]

To understand the charge transfer and interfacial dipole induced by adsorption, the distribution of charge difference $\Delta\rho(z)$ has been obtained using the same method described in the previous work.[11] The distributions $\Delta\rho(z)$ obtained using the PBE-D scheme are demonstrated in Figure 8a,b for the PQ and PMDA molecules on a graphene nanosheet, respectively. From Figure 8, one can see that the strong physisorption induces a small charge transfer. The interfacial dipole p_z due to the redistributed charge densities was calculated by

$$p_z = A\int_{-L_z/2}^{L_z/2} z\Delta\rho(z)\mathrm{d}z \quad (3)$$

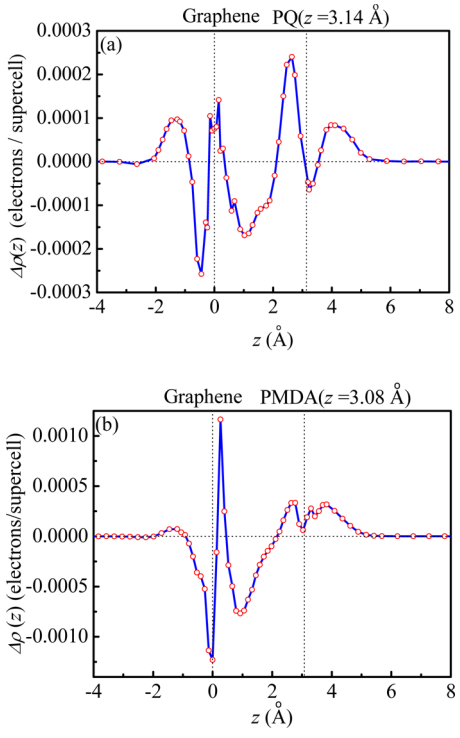

Figure 8. Electron density difference $\Delta\rho(z)$ for (a) the PQ−graphene and (b) PMDA−graphene systems. The vertical dotted lines at z = 0, 3.14 and 3.08 Å are the positions of the monolayer, PQ and PMDA molecules, respectively.

where A is the surface area in xy-plane of the supercell and L_z is the length of the graphene supercell along z-direction. The obtained interfacial dipole moments are listed in Table 3. The absolute values of the interfacial dipole moments for the eight organic molecule−graphene composites are in the range of 0.19−1.20 D.

Work Function. Because the work function change is partly due to the electrostatic interactions, the averaged electrostatic potentials $\phi(z)$ for the PQ−graphene and PMDA−graphene systems are illustrated in Figure 9a,b, respectively. It can be seen in Figure 9 that there are two negative peaks on the curves of electrostatic potentials, and the strong and weak peaks correspond the positions of the graphene nanosheet and organic molecules, respectively. The difference of the electrostatic potential between Fermi and vacuum levels is the work function, which has been calculated and listed in Table 3. The vdW dispersion has a very small contribution (i.e., −0.02 to +0.06 eV) to the work function for eight organic compound−graphene nanocomposites. This agrees quite well with the previous results for the AQ−graphene nanocomposites.[11] The work functions are in the following order: PQ ≈ BDFD ≈ BDTQ < PMDI < PAD < PMDA ≈ PMDT < ATO for both cases of calculations.

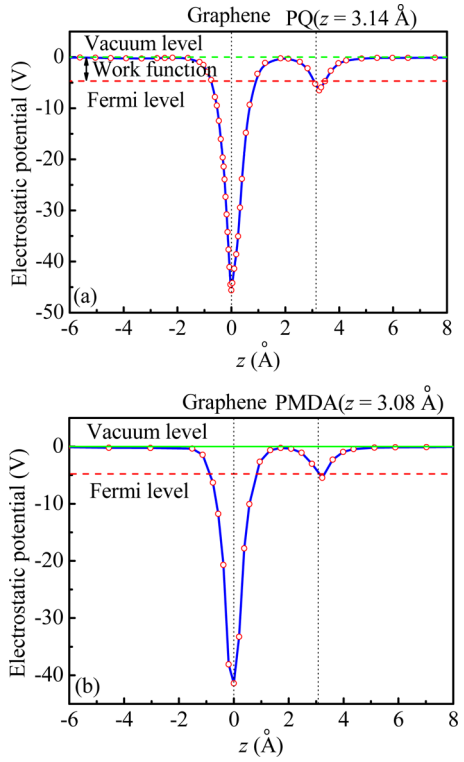

Figure 9. Electrostatic potentials $\phi(z)$ for (a) the PQ and (b) PMDA molecules adsorbed on a graphene nanosheet. The meaning of vertical dotted lines is the same as in Figure 8.

To acquire a quantitative understanding of work function change from the interfacial dipole and the variation of the Fermi level of the intrinsic bulk case, an expression for work function of an organic molecule−graphene nanocomposite has been proposed in the previous work. It is in the following form:[11]

$$\mathrm{WF} = \mu_{\mathrm{M+sheet}} - ep_z/(A\varepsilon_0) \quad (4)$$

where $\mu_{M+sheet}$ is the electron chemical potential for a nanocomposite, and ε_0 is dielectric constant in a vacuum. In this work, the electron chemical potential for the nanocomposite was evaluated from those of the corresponding adsorbate and substrate in a way similar to the chemical potential of a mixed ideal gas.

$$\mathrm{WF} = \frac{A_M \cdot W_M + A \cdot W_G}{A_M + A} - \frac{ep_z}{A\varepsilon_0} \quad (5)$$

where A_M is the sectional area of the organic molecule, and W_M and W_G are the work functions of the isolated organic molecule and pristine graphene, respectively. The values of W_M can be found in Table 1 for the eight organic molecules. The work function W_G = 4.49 eV has been obtained in the previous work.[11] This value of work function of graphene agrees quite well with the experimental value from Yu et al.[29] The sectional areas of an organic molecule can be evaluated as a summation of the sectional area of each atom, i.e., $A_M = \sum \nu_i A_i$, where ν_i and A_i are the number and sectional area of atom i in the organic molecule. In this work, A_i is calculated according to the bond length involving the atom i in the organic molecule. As a result, we have $A_N \approx A_O(\mathrm{C—O—C}) \approx A_C$, $A_O(\mathrm{C{=}O}) = 0.56A_C$, $A_S = 2.56A_C$, $A_H(\mathrm{C—H}) = 0.32A_C$ and $A_H(\mathrm{N—H}) = 0.21A_C$. When A_M tends to zero, eq 5 reduces to an work function equation given by Wigner and Bardeen.[30,31]

The work functions evaluated using eq 5 are compared with those using the PBE-D scheme in Figure 10. It can be seen in Figure 10 that the maximum deviation between the work functions using eq 5 and the PBE-D scheme is within ±0.05 eV. Considering the uncertainty in the calculation of the work function and interfacial dipole moment using the PBE-D scheme, the prediction using eq 5 is very good for the work function of the monolayer adsorption complex. For the multilayer adsorption, adsorption kinetics for different layers should be considered.

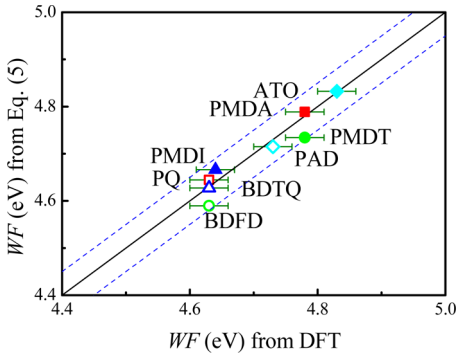

Figure 10. Comparison of the calculated work functions using eq 5 with those using the PBE-D scheme. The upper and lower dashed lines represent the absolute deviation of ±0.05 eV for the work functions. The error bars denote ±0.03 eV, the smallest uncertainty using the PBE-D scheme.

The work function seems to have no apparent link to the capacity of the battery. However, in organic light emitting transistors, a material having a lower work function is suitable to the electron injection electrodes whereas that having a higher work function can be used for the hole injection electrodes.

CONCLUSIONS

The adsorption of the PQ, BDFD, BDTQ, PAD, PMDA, PMDT, PMDI and ATO molecules on graphene has been investigated using ab initio DFT with/without a vdW dispersion correction. The binding energies of the eight organic molecules on graphene are between 1.095 and 1.564 eV, and in the following order: BDFD < BDTQ < PMDA ≤ PMDI < PMDT < PQ < PAD < ATO. The vdW dispersion shortens the equilibrium vertical distances by 0.59−0.78 Å. The contributions of the vdW dispersion to the binding energies are in the range of 0.84−1.20 eV, which are 76.6−80.3% of the total attractive interaction for the organic compound−graphene nanocomposites. The calculated binding energies indicate that the PQ, PMDA and their derivatives can be combined with a graphene nanosheet, preventing the organic molecules dissolved in electrolyte and thereby improving the battery cycle life. The theoretical results suggest that the addition of graphene to the materials containing functional groups quinone and anhydride is a good way to improve organic electrode materials.

The strong physisorption induces a redistribution of charge and hence an interfacial dipole, which contributes a portion to the work function. From the comparison of the work functions in the two calculation cases, we found that the vdW dispersion contributes a very small portion to the work function. The obtained work functions are in the following order: PQ ≈ BDFD ≈ BDTQ < PMDI < PAD < PMDA ≈ PMDT < ATO. A novel relationship between the interfacial dipole and work function has been established and validated. Both the interfacial dipole and the change of the location of the Fermi level are important for the work function. The proposed relationship predicts an accurate work function when compared with the PBE-D scheme. It is very useful in the prediction of the work function for a monolayer adsorption complex.

ASSOCIATED CONTENT

Supporting Information

Optimized geometric structures for adsorption of the eight organic molecules on monolayer graphene. This material is available free of charge via the Internet at http://pubs.acs.org.

AUTHOR INFORMATION

Corresponding Author

*Y.-X. Yu. E-mail: yangxyu@mail.tsinghua.edu.cn. Phone: +86-10-62782558. Fax: +86-10-62770304.

Notes

The authors declare no competing financial interest.

ACKNOWLEDGMENTS

I was greatly indebted to Ms. Yong-Jun Du for her arduous efforts and helps in recording the computed data and in the preparation of the paper. Financial assistance provided by the National Natural Science Foundation of China (no. 21376131) is also highly appreciated.

REFERENCES

(1) Dum, B.; Kamath, H.; Tarascon, J. M. Electrical Energy Storage for the Grid: A Battery of Choices. *Science* **2011**, *334*, 928−935.

(2) Yu, Y.-X. Can All Nitrogen-Doped Defects Improve the Performance of Graphene Anode Materials for Lithium-Ion Batteries? *Phys. Chem. Chem. Phys.* **2013**, *15*, 16819−16827.

(3) Wang, R. H.; Xu, C. H.; Sun, J.; Gao, L.; Yao, H. L. Solvothermal-Induced 3D Macroscopic SnO_2/Nitrogen-Doped Graphene Aerogels for High Capacity and Long-Life Lithium Storage. *ACS Appl. Mater. Interfaces* **2014**, *6*, 3427−3436.
(4) Valavanidis, A.; Vlachogianni, T. Metal Pollution in Ecosystems. Ecotoxicology Studies and Risk Assessment in the Marine Environment. *Science Advances on Environment, Toxicology & Ecotoxicology Issues* [Online], 2010. http://chem-tox-ecotox.org/wp/?p=394.
(5) Forster, U.; Whittmann, G. T. W. *Metal Pollution in the Aquatic Environment*; Springer-Verlag: Berlin, 1983.
(6) Meria, E. E. *Metals and Their Compounds in the Environment Occurrence, Analysis and Bidogical Relevance*; Verlag Chemie: New York, 1991.
(7) Tarascon, J.-M.; Armand, M. Issues and Challenges Facing Rechargeable Lithium Batteries. *Nature* **2001**, *414*, 359−367.
(8) Armand, M.; Tarascon, J.-M. Building Better Batteries. *Nature* **2008**, *451*, 652−657.
(9) Foos, J. S.; Erker, S. M.; Rembetsy, L. M. Synthesis and Characterization of Semiconductive Poly-1,4-dimethoxybenzene and Its Derived Polyquinone. *J. Electrochem. Soc.* **1986**, *133*, 836−841.
(10) Song, Z. P.; Xu, T.; Gordin, M. L.; Jiang, Y.-B.; Bae, I.-T.; Xia, Q. F.; Zhan, H.; Liu, J.; Wang, D. H. Polymer-Graphene Nanocomposites as Ultrafast-Charge and Discharge Cathodes for Rechargeable Lithium Batteries. *Nano Lett.* **2012**, *12*, 2205−2211.
(11) Yu, Y.-X. A Dispersion-Corrected DFT Study on Adsorption of Battery Materials Anthraquinone and Its Derivatives on Monolayer Graphene and h-BN. *J. Mater. Chem. A* **2014**, *2*, 8910−8917.
(12) Liang, Y. L.; Zhang, P.; Yang, S. Q.; Tao, Z. L.; Chen, J. Fused Herteroaromatic Organic Compounds for High-Power Electrodes of Rechargeable Lithium Batteries. *Adv. Energy Mater.* **2013**, *3*, 600−605.
(13) Trasatti, S. The Absolute Electrode Potential: An Explanatory Note (Recommendations 1986). *Pure Appl. Chem.* **1986**, *58*, 955−966.
(14) Grob, A. The Virtual Chemistry Lab for Reactions at Surfaces: Is It Possible? Will It Be Useful? *Surf. Sci.* **2002**, *500*, 347−367.
(15) Yu, Y.-X. Graphenylene: A Promising Anode Material for Lithium-Ion Batteries with High Mobility and Storage. *J. Mater. Chem. A* **2013**, *1*, 13559−13566.
(16) Grimme, S. Semiempirical GGA-Type Density Functional Constructed with a Long-Range Dispersion Correction. *J. Comput. Chem.* **2006**, *27*, 1787−1799.
(17) Delley, B. Fast Calculation of Electrostatics in Crystals and Large Molecules. *J. Phys. Chem.* **1996**, *100*, 6107−6110.
(18) Delley, B. From Molecules to Solids with the $Dmol^3$ Approach. *J. Chem. Phys.* **2000**, *113*, 7756−7764.
(19) Perdew, J. P.; Burke, K.; Ernzerhof, M. Generalized Gradient Approximation Made Simple. *Phys. Rev. Lett.* **1996**, *77*, 3865−3868.
(20) Becke, A. D. Density Functional Thermochemistry. III. The Role of Exact Exchange. *J. Chem. Phys.* **1993**, *98*, 5648−5652.
(21) Cooper, J. K.; Grant, C. D.; Zhang, J. Z. *Ab Initio* Calculation of Ionization Potential and Electron Affinity of Six Common Explosive Compounds. *Rep. Theor. Chem.* **2012**, *1*, 11−19.
(22) Kittel, C. *Introduction to Solid State Physics*, 7th ed.; Wiley: New York, 1996.
(23) Zhang, G.; Musgrave, C. B. Comparison of DFT Methods for Molecular Orbital Eigenvalue Calculations. *J. Phys. Chem. A* **2007**, *111*, 1554−1561.
(24) Pitt, D. A.; Smyth, C. P. Microwave Absorption and Molecular Structure in Liquids XXVII. The Mutual Viscosities and Dielectric Relaxtion Times of Several Polar Aromatic Compounds in Solutions. *J. Am. Chem. Soc.* **1959**, *81*, 783−786.
(25) Potapov, V. K.; Sorokin, V. V. Photoionization and Ion−Molecule Reactions in Quinones and Alcohols. *High Energy Chem.* **1971**, *5*, 435−440.
(26) Botana, E.; Da Silva, E.; Benet-Buchholz, J.; Ballester, P.; de Mendoza, J. Inclusion of Cavitands and Calix[4]arenes into a Metallobridged Para-(1H-imidazo[4,5-f][3,8]phenanthrolin-2-yl)-Expanded Calix[4]arene. *Angew. Chem., Int. Ed* **2007**, *46*, 198−201.
(27) Sakai, M. Pyromellitic Dianhydride (PMDA). *J. Synth. Org. Chem., Jpn.* **1992**, *50*, 659−660.
(28) Lawton, E. A.; McRitche, D. D. Synthesis of Pyromellitonitrile and Related Compounds. *J. Org. Chem.* **1959**, *24*, 26−28.
(29) Yu, Y.-J.; Zhao, Y.; Ryu, S.; Brus, L. E.; Kim, K. S.; Kim, P. Tuning the Graphene Work Function by Electric Field Effect. *Nano Lett.* **2009**, *9*, 3430−3434.
(30) Wigner, E.; Bardeen, J. Theory of the Work Functions of Monovalent Metals. *Phys. Rev.* **1935**, *48*, 84−87.
(31) Lang, N. D.; Kohn, W. Theory of Metal Surfaces: Work Function. *Phys. Rev. B* **1971**, *3*, 1215−1223.